*Pharmaceutical Research, Vol. 22, No. 8, August 2005 (© 2005)*
DOI: 10.1007/s11095-005-5275-7

*Research Paper*

# Effect of Salt Type on Hygroscopicity of a New Cephalosporin S-3578

**Kohsaku Kawakami,[1,3,4] Yasuo Ida,[1] and Tohru Yamaguchi[2]**

*Received January 17, 2005; accepted March 25, 2005*

***Purpose.*** Effect of salt type on hygroscopicity was evaluated using S-3578 salts.
***Methods.*** The hydration behavior of a sulfate and a nitrate salt of S-3578 were evaluated by powder X-ray diffraction (PXRD), simultaneous measurement of PXRD—differential scanning calorimetry (DSC), moisture sorption analysis, simultaneous measurement of thermogravimetric/differential thermal analyses, and solid state $^{13}$C-nuclear magnetic resonance (C-NMR).
***Results.*** The sulfate salt incorporated two types of lattice water to form a monohydrate or a trihydrate. Additional water could also be absorbed as channel water to expand the lattice structure. The activation energy for dehydration was very high, probably due to steric hindrance in the lattice structure. The nitrate salt incorporated only one water molecule per compound as the lattice water. The additional water was absorbed as channel water as observed for the sulfate salt. X-ray diffractograms showed little dependence on the salt type under the ambient condition. The hydration number was likely to be affected by the size of the counter acids.
***Conclusions.*** The hygroscopicity of S-3578 salts was significantly altered by the salt type. The difference in the amount of the lattice water could be explained in terms of the difference in the molecular size of the counter acids.

**KEY WORDS:** activation energy; channel water; dehydration; desorption; hydration; lattice water; salt; sorption.

## INTRODUCTION

Pharmaceutical solids frequently absorb water molecules in their bulk structure and/or adsorb them on their surfaces (1–3). Such hygroscopic behavior needs to be well understood, because it affects many physicochemical characteristics such as purity, solubility, chemical stability, density, surface area, powder flow, compactability, and crystal form (1,3–5). The absorbed water can further be differentiated into lattice water, channel water, and clathrate. The stoichiometric water uptake is usually regarded as lattice water incorporation (1,3,6). Because this water participates in the formation of the lattice structure, its uptake or removal causes change in the crystal form. On the other hand, nonstoichiometric water uptake can be explained in terms of adsorption, heterogeneous hydration, channel water, or clathrate. Differentiating these waters is very difficult in many cases.

Hygroscopic behavior of antibiotics is of great interest among pharmaceutical scientists, because water sorption behavior is usually complicated (6–10). Therefore, many case studies have been reported in literature, and most of them are discussed as abnormal examples. In addition, information on the interaction between β-lactam antibiotics and water is very important, because hydrolysis of β-lactam ring leads to loss in the activity. S-3578 (Fig. 1) is a new broad-spectrum cephalosporin, which has potent activity against both methicillin-resistant *Staphylococcus aureus* and *Pseudomonas aeruginosa* (11). The hygroscopic behavior of this compound was found to be another abnormal example.

A major concern of this article is the effect of the salt type on the hygroscopicity, which may become a critical factor for the developmental study, because it may affect the solid state stability significantly (12,13). Although there are some guidelines for selecting the salt type, it still relies on experience basically. Presented in this article is the effect of size of the counter acids on the hygroscopic behavior, which may become useful information for the salt selection process in some cases.

## MATERIALS AND METHODS

### Materials

S-3578 salts were obtained from Shionogi & Co., Ltd. (Osaka, Japan). In the case of the sulfate salt, one sulfuric acid was required per one compound, while two acid

[1] Developmental Research Laboratories, Shionogi & Co., Ltd., 12-4 Sagisu 5-chome, Fukushima-ku, Osaka 553-0002, Japan.
[2] Discovery Research Laboratories, Shionogi & Co., Ltd., 12-4 Sagisu 5-chome, Fukushima-ku, Osaka 553-0002, Japan.
[3] Present address: Pharmaceutical Research and Development, Banyu Pharmaceutical Co., Ltd., 810 Nishijo, Menuma-machi, Saitama 360-0214, Japan.
[4] To whom correspondence should be addressed. (e-mail: kohsaku_kawakami@merck.com)

**ABBREVIATIONS:** DSC, differential scanning calorimetry; DTA, differential thermal analysis; NMR, nuclear magnetic resonance; PXRD, powder X-ray diffraction; RH, relative humidity; TGA, thermogravimetric analysis.

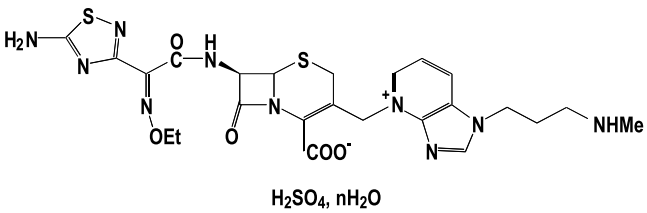


**Fig. 1.** Molecular structure of S-3578 (sulfate salt).

molecules were used for nitrate, hydrochloric, and hydrogen bromic acids. The number of the acid molecules are not described in the text, for example dinitrate salt is simply expressed as nitrate salt. The ratio of salt to the compound was proved by elemental analysis. Amorphous solids of the sulfate and the nitrate salts were obtained with a freeze dryer RL-60BS (Kyowa Corp., Tokyo, Japan). A 1 wt% aqueous solution was frozen at −40°C for 2 h and subjected to primary drying at 10°C for 24 h, followed by secondary drying at 25°C for 5 h. The pressure was reduced to 30 μm Hg. The vials were sealed under nitrogen atmosphere in the freeze dryer and stored at −20°C before use. The amorphicity of the freeze-dried material was confirmed by powder X-ray diffraction (PXRD). All reagents used were of the highest purity available and used as supplied.

### Powder X-ray Diffraction

PXRD patterns were measured by the Rigaku RINT 2000 X-ray Diffraction System (Rigaku Denki, Tokyo, Japan) using CuKα radiation. The voltage and the current were 40 kV and 30 mA, respectively. About 30 mg of sample was loaded into the circle-shaped aluminum pan with a diameter of 10 mm and its surface was smoothed. The data were collected between 5° and 35° (2θ values) at intervals of 0.02° with a scan speed of 4°/min.

For the measurements in which the relative humidity (RH) was precisely controlled, a humidity controller HUM-1A (Rigaku Denki, Tokyo, Japan) was attached to a sample stage of Thermo Plus II (Rigaku Denki, Tokyo, Japan), which was used to enclose the sample atmosphere. About 10 mg of sample was loaded into the square-shaped aluminum pan with an axis of 10 mm and its surface was smoothed. The desired relative humidity was produced by mixing water vapor and dry air at various ratios. The flow rate of the air was in the range of 350–450 ml/min. The voltage and the current were 40 kV and 40 mA, respectively.

### Simultaneous Measurement of PXRD and Differential Scanning Calorimetry (XRD–DSC)

XRD–DSC measurements were also performed on the Rigaku RINT 2000 X-ray Diffraction System with Thermo Plus II DSC unit (Rigaku Denki, Tokyo, Japan). About 10 mg of sample was loaded into the square-shaped aluminum pan as described above. The voltage and the current were 40 kV and 40 mA, respectively. The heating rate was 2°C/min. The X-ray data were collected between 5° and 40° (2 theta values) at intervals of 0.02° with a scan speed of 7°/min. RH was not controlled in this study.

### Water Vapor Sorption and Desorption

The weight change associated with the water vapor sorption and desorption was monitored with an IGAsorp moisture sorption analyzer (Hiden Analyticals, London, UK). The instrument was calibrated using a 100-mg weight (for weight) and lithium chloride, potassium carbonate, and sodium chloride [for relative humidity (RH)]. About 10 mg of the sample was loaded in a meshed basket and exposed to dry air (3.5% RH) at the flow rate of 490 ml/min until the weight became constant. Typically, 6–8 h were required for this procedure. In the measurement, stepwise increments of RH, which was controlled by mixing water vapor and dry air, were applied at intervals of 5% RH. Under each RH condition, the weight change of the sample was investigated at least for 10 min, and the observed weight, $w$, was fitted to the exponential decay function:

$$\frac{w_e - w}{w_e - w_i} = \exp\left(-\frac{t}{\tau}\right) \quad (1)$$

where $w_i$ and $w_e$ are the initial and the equilibrium weight, respectively, and $t$ and $\tau$ are time and a decay constant, respectively. This fitting procedure was automatically performed using the operating software. Data collection was finished when 98% of the sorption was attained, that is, when $(w_e - w)/(w_e - w_i)$ became smaller than 0.02. The values of $w_e$ were employed as the final data. The $w_e$ data was obtained within 3 h at all the RH conditions. When 90% RH was reached, the desorption process was investigated in the same manner by decreasing RH at intervals of 5%.

Because the procedure described above provides only the weight change associated with water sorption and desorption, it does not directly give the hydration number. To determine this, thermogravimetric analysis and Karl Fisher measurement were performed. Details of the thermogravimetric analysis are given later. RH around the instrument was measured by Humidex YH-12 (Yamato Scientific Co., Tokyo, Japan). Karl-Fisher Moisture Titrator MKS-510N (Kyoto Electronics Manufacturing Co., Kyoto, Japan) was used for the Karl Fisher measurements. The samples for this measurement were stored in desiccators for 1 day at 25°C, in which saturated salt solutions were filled to control RH. The salts employed to control RH were lithium chloride (11% RH), magnesium chloride (33% RH), and magnesium nitrate (52% RH). The chemical stability of the compound under a humid atmosphere was assured in preliminary experiments. The equilibrated samples were transferred to a volumetric flask in a dry box, in which RH was controlled by bubbling the same saturated salt solutions used for the desiccators. The samples were dispersed in methanol, followed by filtration using syringe filters. The filtrate was subjected to the water content analysis.

### Simultaneous Measurement of Thermogravimetric Analysis (TGA) and Differential Thermal Analysis (DTA)

Simultaneous measurement of TGA weight change and DTA heat flow was performed on Seiko TG/DTA 220U (Seiko Instruments, Tokyo, Japan) with various scan rates. The instrument was calibrated with indium and calcium chloride. About 5 mg of the sample was loaded into an

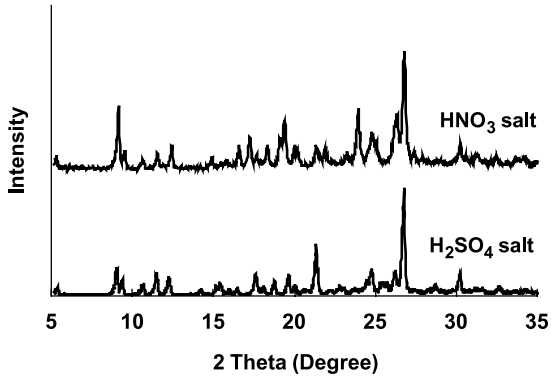


**Fig. 2.** PXRD patterns of the sulfate and the nitrate salts of S-3578 at ambient condition (25°C, 40–50% RH).

aluminum open pan with a diameter of 5 mm and analyzed under a flow of dry air at 100 ml/min. Precise quantification of the sorbed water was done (Fig. 4) without the flow of dry air to avoid desorption before measurement, from which the data were used to convert the hygroscopicity data to the hydration number as described above.

### Solid-State $^{13}$C-Nuclear Magnetic Resonance (C-NMR)

$^{13}$C cross polarization/magic angle spinning (CP/MAS) spectra were acquired on a Varian Unity Inova500 spectrometer equipped with a CP/MAS probe (Varian Inc., Palo Alto, CA) with a standard CP pulse sequence. The water content of the NMR samples was controlled by storing the sample in desiccators equilibrated with the saturated salt solutions. About 100 mg of sample was transferred to a silicon nitride rotor (5 mm ID × 20 mm L) in a RH-controlled dry box as done for the Karl Fisher measurements.

## RESULTS AND DISCUSSION

### Basic Physical Characteristics of S-3578 Salts under Ambient Condition

Figure 2 shows X-ray diffraction patterns of the sulfate and the nitrate salt at ambient condition. As can be seen, there were only small differences in the diffraction patterns. Therefore, the lattice structures of these salts do not seem to differ greatly. Figure 3 shows the results of the simultaneous measurements of TGA and DTA at the heating rate of 2°C/min. The total hydration numbers of the sulfate and the nitrate salts were determined as 5.2 and 2.9, respectively. However, it should be noted that these results are likely to be slightly underestimated, because dehydration can occur under the flow of dry air even at the ambient temperature. In other words, precise determination of the hydration number of compounds, which release water easily at ambient temperature, is sometimes difficult with dry air as the purge gas. The sulfate salt exhibited three strong endothermic peaks at 37°C, 57°C, and 71°C. The decrease in the weight proved that these peaks were due to the loss of 2.2, 2, and 1 water molecules, respectively, although the precise discrimination of these events was difficult. An additional small peak at 120°C was also observed. Because the weight decrease was not associated with this peak, it was not due to the dehydration. Therefore, the most likely interpretation of this peak is enantiotropically related polymorphic transition (14). This is discussed further in the XRD–DSC measurement section. As for the nitrate salt, two broad endothermic peaks were observed at 56 and 78°C, which were due to the loss of 1.9 and 1 water molecules, respectively.

### Hygroscopic Properties of S-3578 Salts at Ambient Temperature

Figure 4 shows the hygroscopic properties of the sulfate and the nitrate salts at 25°C. Because the automatic moisture analyzer does not provide direct information on the hydration number, TGA and Karl Fisher measurements were also performed. These experiments showed that neither salt was dehydrated completely but still held one water molecule at 3% RH, because results from the three methods agreed very well with each other under this assumption. No hysteresis was observed for the two salts.

The weight of the sulfate salt showed stepwise increase with an increase in RH below 40%, followed by a gradual increase above that RH. The stepwise increase is usually attributed to the lattice water and the gradual increase to the channel water or adsorbed water. The stoichiometric water is usually thought of as the lattice water, and the nonstoichiometric water as the channel water, the clathrates, or the adsorbed water (the issue of heterogeneity is ignored here for

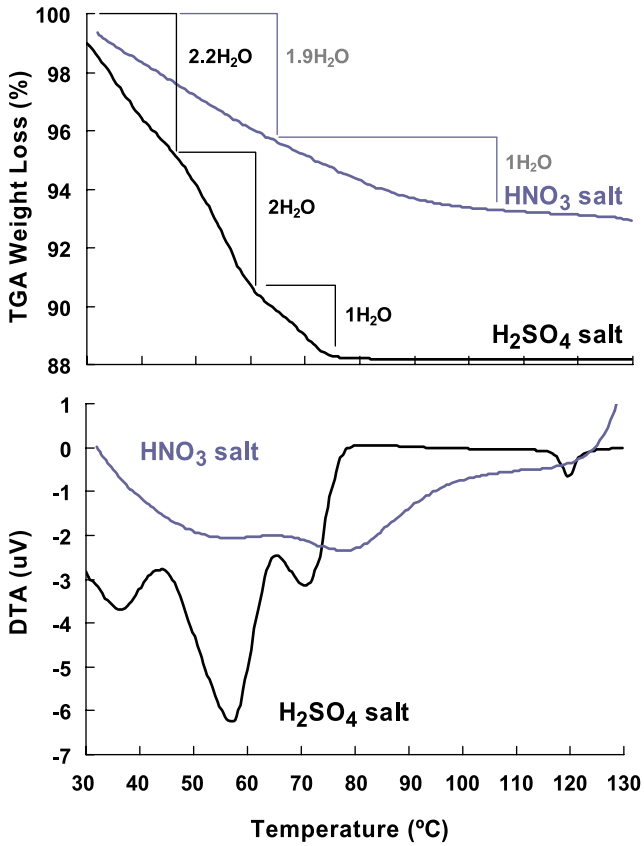


**Fig. 3.** Simultaneous analysis of TGA and DTA of S-3578 salts. The heating rate was 2°C/min. Black and gray lines represent the sulfate and the nitrate salts, respectively. The calculated number of dehydrated water molecules is also indicated in the figure.

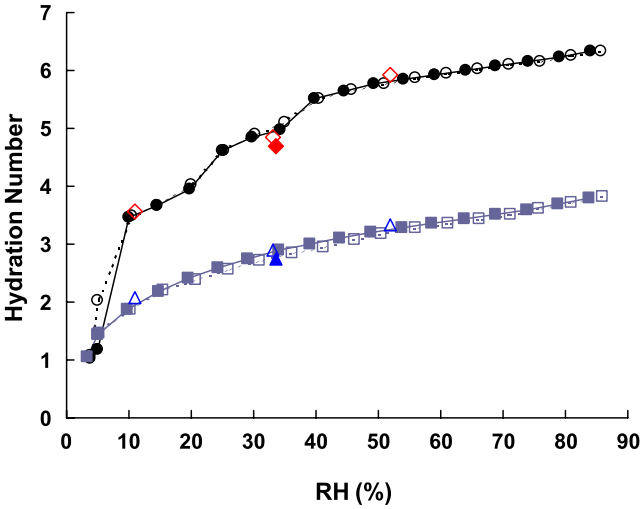


**Fig. 4.** Water sorption/desorption isotherm of S-3578 salts at 25°C. The sorption processes are shown as closed symbols and connected by solid lines. The desorption processes are shown as open symbols and connected by dashed lines. These two processes were consistent each other for both salts. Sulfate and nitrate salts are expressed as circles and squares, respectively. Results of Karl Fisher analysis are presented for sulfate and nitrate salts as open diamonds and open triangles, respectively. Those of TGA are given as closed diamonds and closed triangles, respectively.

simplicity). Based on this knowledge and the results of the TGA and DTA, $1H_2O$ held at RH 3% seemed to be the lattice water. The $3.5H_2O$ at RH 10% seemed to be separable into three lattice waters and other waters. The two steps at higher RHs were too small to interpret as lattice water, although nonstoichiometric hydration as lattice water is also possible. This is discussed further later.

As for the nitrate salt, the weight increased gradually in the entire RH range investigated. The total amount of sorbed water was much lower than that of the sulfate salt. The $1H_2O$ at RH 3% seemed to be the lattice water as in the case of the sulfate salt. The gradual increase of the water above that RH seemed to be due to channel water, because the amount of adsorbed water is generally less than 1%, which corresponds to only $0.4H_2O$ for this salt. Detailed discussion on this will be presented again.

## PXRD Patterns at Various RH Conditions

Figure 5 shows the PXRD patterns of the sulfate salt at various RH conditions. As can be seen, a change in the diffraction pattern was observed between 3% and 10% RH. Therefore, change in the crystal form seemed to occur between these RH levels. This observation supports the assumption made in the previous section, that is, the lattice water is incorporated between these RH levels. Above 10% RH, the diffraction patterns were basically the same, except that some peaks shifted to lower degrees with the increase in RH. The most striking shift was observed for the peak indicated by the arrow in the figure; it moved from 26.74° (10% RH) to 26.44° (50% RH). Therefore, the channel water is most likely to be taken up in this RH range to expand the lattice structure.

Figure 6 shows the PXRD patterns of the nitrate salt at various RH conditions. The change in the diffraction pattern was observed between 3% and 10% RH levels. This result does not seem to be consistent with the observation made in the hygroscopicity measurement, because only a gradual increase in the amount of the sorbed water was observed in this RH range. However, the XRD-DSC result shown later suggested that the hydration number might be less than one in this experiment, because this diffraction pattern at RH 3% was consistent with the pattern of the anhydrate in that analysis. This discrepancy was most likely to be caused by a difference in the experimental conditions such as the flow rate of the dry air and whether the samples were compressed or not. The shift of some diffraction peaks to a lower degree was observed between 10% and 50% RH levels, suggesting that the channel water was incorporated in this RH range. The most striking shift was observed for the peak indicated by the arrow in the figure, which moved from 26.72° (10% RH) to 26.42° (50% RH). Because this observation was very similar to that for the sulfate salt, the water molecules above $3H_2O$ for the sulfate salt and those above $1H_2O$ for the

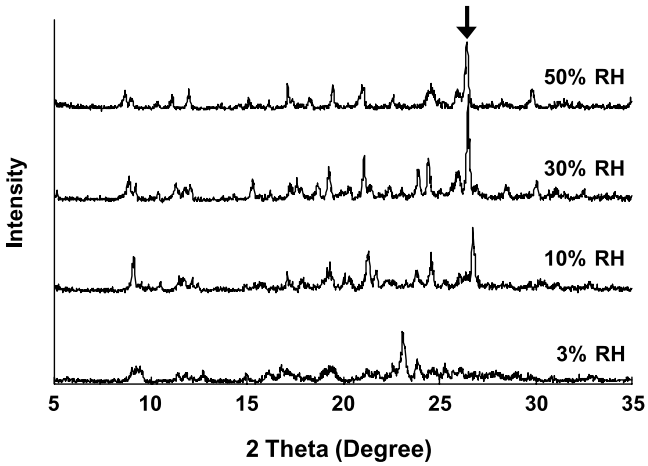


**Fig. 5.** PXRD patterns of the sulfate salt at various humidity conditions as shown in the figure. Explanation of the arrow is described in the text.

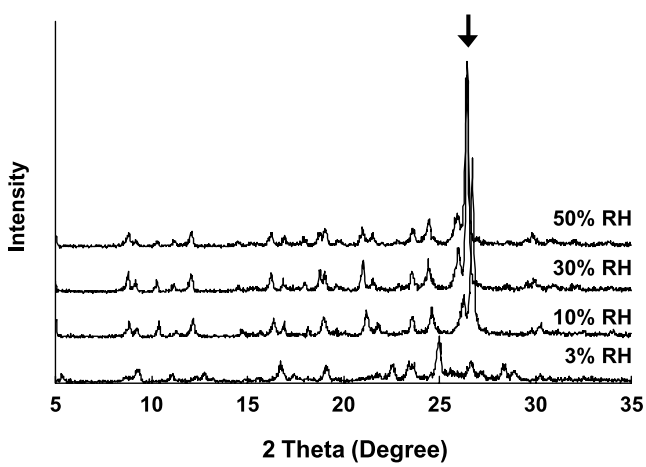


**Fig. 6.** PXRD patterns of the nitrate salt at various humidity conditions as shown in the figure. Explanation of the arrow is described in the text.

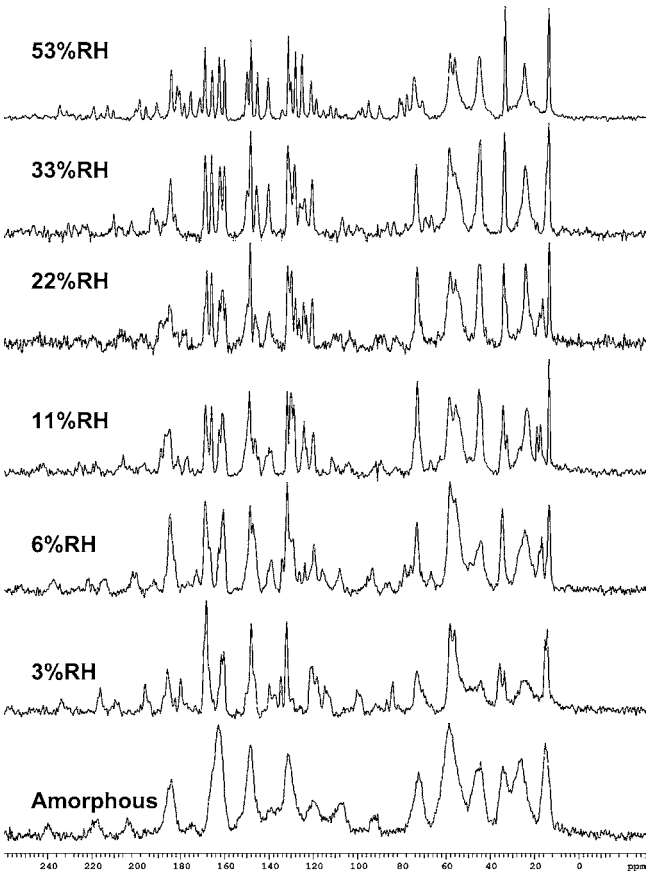


**Fig. 7.** C-NMR spectrum of the sulfate salt under various humidity conditions as shown in the figure.

nitrate salt seemed to play the same role in the crystal structure.

### C-NMR Spectra Under Various RH Conditions

Solid-state NMR has been known to offer information on the short-range interactions between atoms (8,15). Figure 7 shows the C-NMR spectra of the sulfate salt under various RH conditions. The spectrum of the amorphous state is also presented for reference; it had very broad peaks as is often the case with amorphous samples (15). Comparison of the spectra led to the conclusion that the spectra at 3% RH differed from the others. The most apparent difference was broadening of signals at 25 and 45 ppm and splitting at 14 and 34 ppm, suggesting that there was a change in the crystal form between 3% and 6% RH levels. This can be elucidated in terms of the transition from $1H_2O$ to $3H_2O$. In addition, two small peaks are observed around 18 ppm only in the range of 6–22% RH. A peak at 34 ppm became split at 11% RH and was absorbed again at 22% RH. The PXRD and the hygroscopicity evaluation suggested that the sulfate salt was a trihydrate but also possesses the channel waters in this RH range. Therefore, these observations seem to be due to the interaction of the sulfate salt with the channel waters. The absence of these peaks at higher RH can be explained by their increased mobility. The broadness of the peaks at 3% RH suggests low crystallinity, because a nucleus in a less structured environment does not give an intense signal due to low efficiency of the cross polarization in a CP/MAS spectrum. The broadness of spinning side bands (signals above 100 ppm), which proves a decrease in anisotropic interactions notably for aromatic and carbonyl carbons, seems to support this assumption as well.

Figure 8 shows C-NMR spectra of the nitrate salt under various RH conditions, together with its amorphous spectrum. Unlike the results for the sulfate salt, all the spectra of the crystals were basically the same, indicating that there were no significant change in the crystal form in this RH range. However, small splitting of the peaks at 16° and 36° were observed only for the spectrum at 3% RH. Based on the assumptions made in the previous experiments, a small amount of the anhydrate form may be present at this RH.

### XRD–DSC Measurements

Figure 9 shows a result of the XRD–DSC measurement of the sulfate salt. In the DSC analysis, three dehydration peaks were observed as for DTA; however, the dehydration temperature was higher than those for DTA. This discrepancy was most likely due to the difference in the sample atmosphere and the preparation procedure. In the XRD–DSC measurements, the samples were heated without the purge gas, while dry air was supplied in the case of DTA. Also, the sample was compressed to form thin films for the XRD–DSC measurements. Therefore, the bulk surface area should have been smaller and the bulk density higher than those of the DTA samples, both of which made the dehydration slower. This measurement revealed that the first dehydration (from $5H_2O$ to $3H_2O$) did not alter the crystal lattice structure but the shift of some peaks to a higher degree was observed. Therefore, the water molecules lost in this step seemed to be the channel water. The shift of the diffraction peaks seemed to be due to the shrinkage of the lattice structure as a result of the loss of the channel water. The second dehydration (from $3H_2O$ to $1H_2O$) did alter the crystal lattice structure.

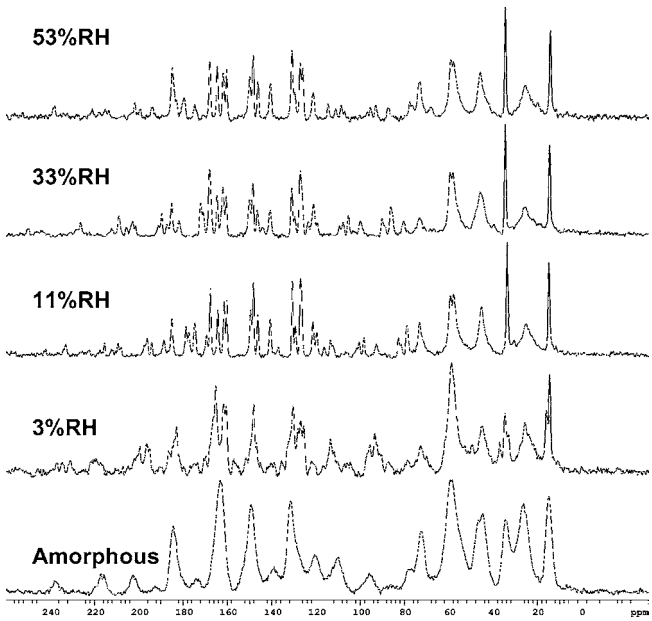


**Fig. 8.** C-NMR spectrum of the nitrate salt under various humidity conditions as shown in the figure.

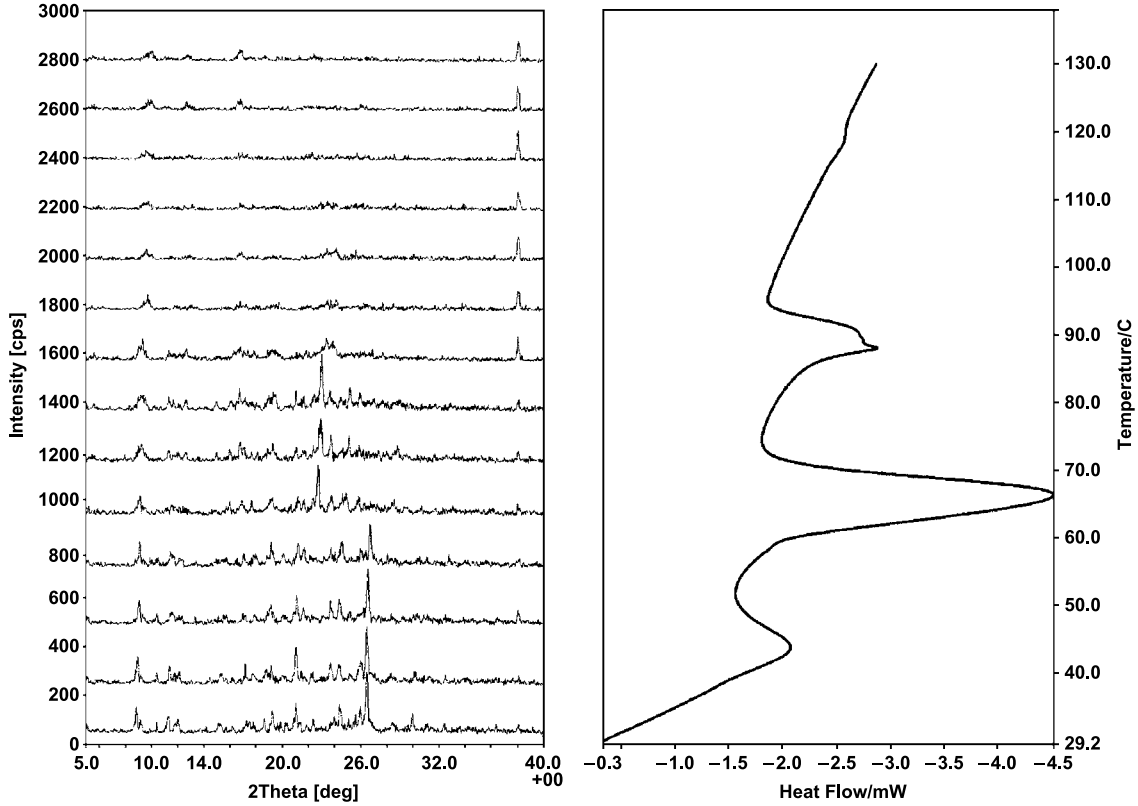


**Fig. 9.** XRD–DSC measurement of the sulfate salt. The heating rate was 2°C/min. The diffraction peak at 38.5° is due to the aluminum sample pan.

Therefore, those water molecules were most likely to be the lattice waters. This interpretation was also applicable for the third dehydration (from $1H_2O$ to $0H_2O$). The small endothermic event at 117°C seemed to be the polymorphic transition, because the growth of two peaks at 14° and 18° was observed above this temperature. Because the endothermic peak is usually an indication of enantiotropic transition (14), this is most likely the transition to the stable form at higher temperature. The melting of a small amount of anhydrate crystal, which has been formed during the heating, may be another possible explanation for this observation.

Figure 10 shows a result of the XRD–DSC measurement of the nitrate salt. Although it was very difficult to recognize dehydration peaks due to their broadness and the small enthalpy, the first dehydration (from $3H_2O$ to $1H_2O$) did not seem to alter the crystal lattice structure and the shift of some peaks to higher degrees was observed. The change in the diffraction pattern was investigated at around 90°C, which was most likely to be due to the second dehydration (from $1H_2O$ to $0H_2O$). The change in the crystal form for both salts with the increase in temperature were totally consistent with the change associated with the decrease in RH. Therefore, the change in the crystal form of both salts was proved to follow the same route for either condition change.

## Further Study on Hygroscopicity of Sulfate Salt

The increase in the hydration number of the sulfate salt from $1H_2O$ to $3H_2O$ with the increase in RH was shown to be due to the incorporation of lattice water. However, Fig. 4 showed that there were also stepwise increases in the hydration number above 10% RH. The next experiment was thus performed to explain why there were small steps in the hydration behavior between 10% and 50% RH levels.

Figure 11 shows the water sorption isotherms at various temperature conditions. As can be seen, two small steps (20–30%RH, 35–40%RH) were observed in the isotherms of 25 and 40°C. However, one of the steps (low-RH side) disappeared from those of 50 and 60°C without affecting the hydration number significantly. Because the water molecules above $3H_2O$ were attributed to the channel water, thermal expansion of the lattice structure at higher temperatures might remove the steric hindrance in the channel structure.

If there is steric hindrance in the channel structure, the activation energy of the dehydration should be large. The activation energy of the dehydration could be estimated by altering the heating rate, $q$, in the DTA analysis and applying Kissinger's plot (16). An equation for this plot can be written as (16,17)

$$\frac{d\ln(q/T_d^2)}{d(1/T_d)} = -\frac{E_a}{R} \qquad (2)$$

where $T_d$ and $E_a$ are the dehydration temperature and the activation energy, respectively. $E_a$ can be determined by plotting $\ln(q/T_d^2)$ against $1/T_d$. Figure 12 shows this plot for the dehydration of the sulfate salt. Strictly speaking, direct information can be obtained by applying this analysis to the channel water, that is, the water above $3H_2O$. However,

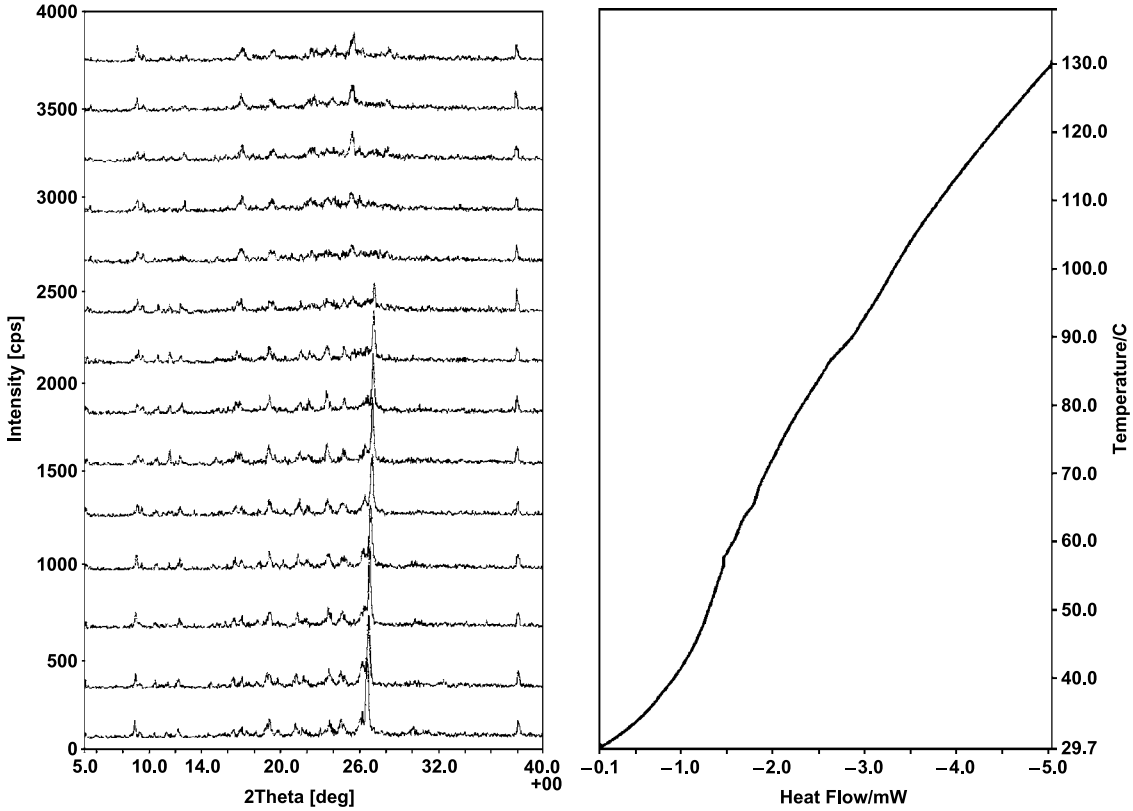


**Fig. 10.** XRD–DSC measurement of the nitrate salt. The heating rate was 2°C/min. The diffraction peak at 38.5° is due to the aluminum sample pan.

because this water is immediately removed under the flow of dry air, precise estimation of the dehydration temperature was difficult. Therefore, we estimated the activation energy for the lattice water, because it was also expected to go through the channel upon dehydration. As for the dehydration from $3H_2O$ to $1H_2O$, this analysis was possible only when $q$ was smaller than 2°C/min, because the dehydration peak overlapped with that for the dehydration from $5H_2O$ to $3H_2O$ under fast heating rates. As can be seen, Kissinger's plot provided good linearity in the heating rate range between 0.7 and 2°C/min with the $E_a$ value of 173 kJ/mol. This value is relatively larger than the typical $E_a$ values (16–21), suggesting that something interfered with the dehydration behavior and thus the contribution of the steric hindrance was very likely. On the other hand, the slope of Kissinger's plot for the dehydration from $1H_2O$ to $0H_2O$ showed strong dependency on the heating rate. When the heating rate was high (5–10°C/min), the activation energy

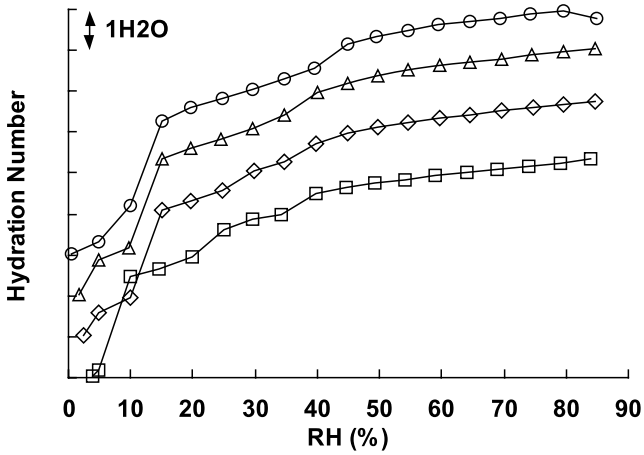


**Fig. 11.** Water sorption isotherms of the sulfate salt. The experimental temperatures are 60, 50, 40, and 25°C (top to bottom), respectively. Because the hydration behaviors did not differ from each other greatly, each isotherm was slid along the $y$-axis for clear comparison.

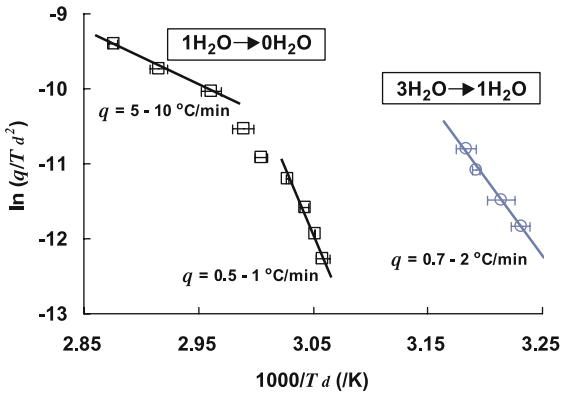


**Fig. 12.** Kissinger's plot of the dehydration process of the sulfate salt. The slope of this plot can be regarded as $-E_a/R$ [Eq. (2)]. The error bars (standard errors) for the $y$-axis direction were omitted, because the range of the error was smaller than the symbols in the figure. The dehydration from trihydrate to monohydrate is shown by the circles, and that from monohydrate to anhydrate by the squares.

**Table I.** Correlation between Hydration Number and MW of Salt (25°C, 40–50% RH)

| Counter salt | MW | Hydration number |
|---|---|---|
| 2HCl | 72.9 | 4.9 |
| $H_2SO_4$ | 98.1 | 5.2 |
| $2HNO_3$ | 126.0 | 2.9 |
| 2HBr | 161.8 | 2.6 |

MW, molecular weight.

was 61.9 kJ/mol, which seems to be a typical value. However, that for the lower heating rate (0.5–1°C/min) was 357 kJ/mol. This large value could also be elucidated in terms of the steric hindrance in the channel structure.

### Impact of Difference in Salt Species on Hygroscopic Property

As presented earlier, the sulfate salt and the nitrate salt seemed to have similar crystal structures at the ambient condition, because the PXRD experiments provided similar diffraction patterns. The hydration number under this condition was approximately 5 for the sulfate salt and 3 for the nitrate salt. This difference was due to a difference in the lattice water number, which was 3 for the sulfate salt but only 1 for the nitrate salt. Here it should be recalled that there is a difference in the number of molecules of counter acid per compound. The difference in the molecular weight between one molecule of the sulfuric acid and two molecules of the nitric acid is 28. Therefore, from the standpoint of the molecular weight, two additional water molecules may fill the space made by the difference in the size between two counter acids. To confirm this hypothesis, hydrochloride salt and hydrogen bromide salt were prepared to observe the hygroscopicity. These salts showed similar PXRD patterns with those of the sulfate and the nitrate salts (data not shown). Table I shows the hydration number of these salts at the ambient condition (25°C, 40–50%RH) determined by TGA. Basically, the increase in the molecular weight of the counter acid reduced the hydration number as expected. The three-dimensional structure of each molecule (counter acid and water) needs to be considered to confirm whether or not the water molecules can account for the difference in the size of the acid molecules. Nevertheless, this simple hypothesis may be applicable to some extent, if a change in the salt type does not alter the crystal structure of the complex significantly. In the salt screening process, hygroscopicity has been regarded as one of the most important characteristics to be evaluated (12,13). The difference in the size of the counter acid may be regarded as one of the indicators affecting the hygroscopicity in the salt selection process of new chemical entities.

## CONCLUSIONS

The hydration behaviors of the sulfate and the nitrate salts of S-3578 were investigated. The sulfate salt incorporated two types of lattice waters, and thus could exist as a monohydrate and a trihydrate. Additional water could also be absorbed as channel water to expand its lattice structure. This channel water seemed to experience steric hindrance in the lattice, leading to unusually high activation energy for the dehydration. The nitrate salt incorporated only one water molecule per compound as the lattice water to alter the crystal form. Additional water was absorbed as channel water as observed for the sulfate salt. Although these salts seemed to have similar crystal structures, there was a remarkable difference in their hygroscopic behavior. The difference in the lattice water number could be explained in terms of the difference in the size of the counter acid.

## REFERENCES


1. G. Zografi. States of water associated with solids. *Drug Dev. Ind. Pharm.* **14**:1905–1926 (1988).
2. J. P. Elder. Thermophysical characterization studies of pharmaceutical hydrates. *Thermochim. Acta* **234**:153–164 (1994).
3. R. K. Khankari and D. J. W. Grant. Pharmaceutical hydrates. *Thermochim. Acta* **248**:61–79 (1995).
4. C. Ahlneck and G. Zografi. The molecular basis of moisture effects on the physical and chemical stability of drugs in the solid state. *Int. J. Pharm.* **62**:87–95 (1990).
5. M. Ono, Y. Tozuka, T. Oguchi, S. Yamamura, and K. Yamamoto. Effects of dehydration temperature on water vapor adsorption and dissolution behavior of carbamazepine. *Int. J. Pharm.* **239**:1–12 (2002).
6. S. M. Reutzel and V. A. Russell. Origins of the unusual hygroscopicity observed in LY297802 tartrate. *J. Pharm. Sci.* **87**:1568–1571 (1998).
7. L. D. Hansen, M. T. Pyne, and R. W. Wood. Water vapor sorption by cephalosporins and penicillins. *Int. J. Pharm.* **137**:1–9 (1996).
8. G. A. Stephenson, J. G. Stowell, P. H. Toma, R. R. Pfeiffer, and S. R. Byrn. Solid-state investigations of erythromycin A dihydrate: structure, NMR spectroscopy, and hygroscopicity. *J. Pharm. Sci.* **86**:1239–1244 (1997).
9. G. A. Stephenson and B. A. Diseroad. Structural relationship and desolvation behavior of cromolyn, cefazolin, and fenoprofen sodium hydrates. *Int. J. Pharm.* **198**:167–177 (2000).
10. H. Mimura, S. Kitamura, T. Kitagawa, and S. Kohda. Characterization of the non-stoichiometric and isomorphic hydration and solvation in FK041 clathrate. *Colloids Surf. B Biointerfaces* **26**:397–406 (2002).
11. H. Yoshizawa, H. Itani, K. Ishikura, T. Irie, K. Yokoo, T. Kubota, K. Minami, T. Iwaki, H. Miwa, and Y. Nishitani. S-3578, a new broad spectrum parenteral cephalosporin exhibiting potent activity against both methicillin-resistant *Staphylococcus aureus* (MRSA) and *Pseudomonas aeruginosa*. Synthesis and structure-activity relationships. *J. Antibiot.* **55**:975–992 (2002).
12. K. R. Morris, M. G. Fakes, A. B. Thakur, A. W. Newman, A. K. Singh, J. J. Venit, C. J. Spagnuolo, and A. T. M. Serajuddin. An integrated approach to the selection of optimal salt form for a new drug candidate. *Int. J. Pharm.* **105**:209–217 (1994).
13. E. C. Ware and D. R. Lu. An automated approach to salt selection for new unique trazodone salts. *Pharm. Res.* **21**:177–184 (2004).
14. K. Kawakami and Y. Ida. Application of modulated-temperature DSC to the analysis of enantiotropically related polymorphic transitions. *Thermochim. Acta* **427**:93–99 (2005).
15. G. A. Stephenson, J. G. Stowell, P. H. Toma, D. E. Dorman, J. R. Greene, and S. R. Byrn. Solid-state analysis of polymorphic, isomorphic, and solvated forms of dirithromycin. *J. Am. Chem. Soc.* **116**:5766–5773 (1994).
16. J. Sheng, G. M. Venkatesh, S. P. Duddu, and D. J. W. Grant. Dehydration behavior of eprosartan mesylate dihydate. *J. Pharm. Sci.* **88**:1021–1029 (1999).
17. H. E. Kissinger. Reaction kinetics in differential thermal analysis. *Anal. Chem.* **29**:1702–1706 (1957).

18. J. Han and R. Suryanarayanan. Applications of pressure differential scanning calorimetry in the study of pharmaceutical hydrates I. Carbamazepine dihydrate. *Int. J. Pharm.* **157**:209–218 (1997).
19. L. S. Taylor and P. York. Effect of particle size and temperature on the dehydration kinetics of trehalose dihydrate. *Int. J. Pharm.* **167**:215–221 (1998).
20. J. Han and R. Suryanarayanan. A method for the rapid evaluation of the physical stability of pharmaceutical hydrates. *Thermochim. Acta* **329**:163–170 (1999).
21. Z. Dong, J. S. Salsbury, D. Zhou, E. J. Munson, S. A. Schroeder, I. Prakash, S. Vyazovkin, C. A. Wight, and D. J. W. Grant. Dehydration kinetics of neotame monohydrate. *J. Pharm. Sci.* **91**:1423–1431 (2002).